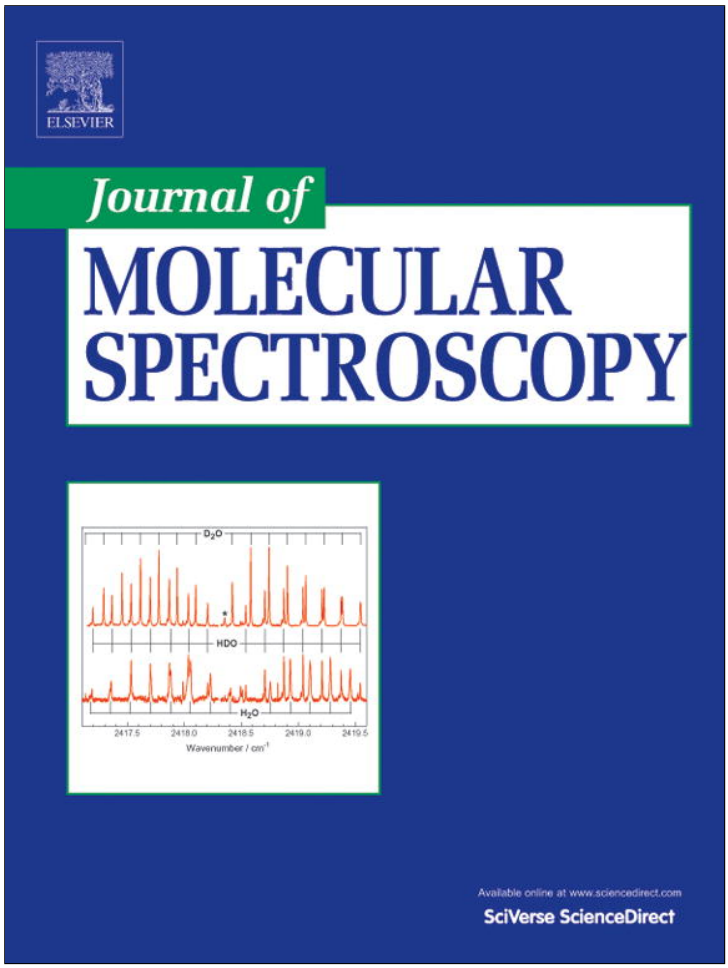

(This is a sample cover image for this issue. The actual cover is not yet available at this time.)

Journal of Molecular Spectroscopy 282 (2012) 20–26

Contents lists available at SciVerse ScienceDirect

Journal of Molecular Spectroscopy

journal homepage: www.elsevier.com/locate/jms

Rydberg and ion-pair states of HBr: New REMPI observations and analysis

Jingming Long, Huasheng Wang, Ágúst Kvaran *

Science Institute, University of Iceland, Dunhagi 3, 107 Reykjavík, Iceland

ARTICLE INFO

Article history:
Received 13 July 2012
In revised form 12 October 2012
Available online 24 October 2012

Keywords:
Rydberg states
Ion-pair states
REMPI
State interactions
Photoionization
Photofragmentation

ABSTRACT

Two-dimensional REMPI data, obtained by recording ion mass spectra for HBr as a function of two-photon wavenumber, revealed previously unobserved $(2+n)$ REMPI spectra for $H^{79}Br$ and $H^{81}Br$. Spectra were assigned and analyzed to derive band origins and rotational parameters of Rydberg and ion-pair states. Perturbation effects, showing as line-shifts and/or signal intensity alterations, were found to be helpful in spectra assignments.

1. Introduction

Vacuum ultraviolet absorption spectra of the hydrogen halides were first reported and studied in 1938 by Price [1]. Since then a wealth of spectroscopic data has been derived from high resolution absorption spectroscopy [2–12], fluorescence studies [12,13], as well as from resonance enhanced multiphoton ionization (REMPI) [14–29]. Largest emphasis has been on studies of HCl [4–6,12,14–20,22,25–27,30] (DCl [4,5]), but studies of HBr [2,3,9,13,21,22,26–29] (DBr [9]) and HI [7,8,11,22–24,26] (DI [7,8,10]) have been significantly less. These studies have revealed and led to characterization of large number of Rydberg states as well as number of vibrational states of the $V^1\Sigma^+$ ion-pair state. Theoretical *ab initio* calculations, to determine excited state potential energy surfaces for HCl [31–33], have proven to be very helpful for interpreting experimental data. Analogous calculations for HBr [34] and HI are more limited.

Whereas most of the studies of the Rydberg and ion-pair states have been dealing with the energetics of the states, an increasing attention has been brought to state interactions, energy transfers and photodissociation processes recently, again with largest emphasis on HCl [35–44]. The hydrogen halide spectra are rich in intensity anomalies and line-shifts due to perturbation effects, which makes them ideal for studying state mixing and photo-fragmentation processes. Interactions between ion-pair vibrational states and Rydberg states, of various strengths, have been seen. These can be grouped into three main categories as,

(a) Very weak near-resonance state interactions, distinguishable by negligible rotational line shifts but significant alterations in signal line intensities [44], observed for triplet Rydberg states and $\Delta\Omega > 0$ state interactions.
(b) Weak near-resonance state interactions, distinguishable by localized line shifts (hence energy level shifts), as well as alterations in signal line intensities [43,45], observed for singlet states and $\Delta\Omega > 0$ state interactions.
(c) Medium to strong off-resonance state interactions, distinguishable by large scale line- and energy-level shifts, as well as alterations in signal intensities [45], observed for $\Delta\Omega = 0$ state interactions.

These characteristics can also be useful in spectra assignments [45,46]. Thus, observations due to near-resonance interactions between states with same J' quantum numbers can be useful to assign rotational transitions to peaks [45,46] and interaction strengths can be decisive about electronic state terms involved [47].

A summary of Rydberg states observed in classical absorption spectra for HBr was given by Ginter et al. in 1981 [9]. A pioneering work by Callaghan and Gordon in 1990 [21] summarizes large number of Rydberg and ion-pair states which have been observed for HBr in REMPI. In 1998 we published a paper with some additional observations for $\Omega = 0$ states of HBr seen in REMPI [26]. Recently we have performed detailed photofragmentation and state interaction studies based on perturbation observations in REMPI seen for resonance excitations to selected Rydberg and ion-pair states of HBr [47]. We will now present two-dimensional REMPI data within the two-photon excitation region 74000–86000 cm^{-1} and interpretations relevant to new spectroscopic identifications.

* Corresponding author. Fax: +354 552 8911.
E-mail address: agust@hi.is (Á. Kvaran).

0022-2852/$ - see front matter © 2012 Elsevier Inc. All rights reserved.
http://dx.doi.org/10.1016/j.jms.2012.10.008

Perturbation effects, showing as line-shifts and/or signal intensity alterations, are found to be very useful in the spectra assignments.

2. Experimental

Two dimensional (2D) REMPI data were recorded for a HBr molecular beam, created by jet expansion of a pure sample through a pulse nozzle. Apparatus used is similar to that described elsewhere [48–50]. Excitation radiation was generated by pulsed excimer laser-pumped dye laser systems, using a Lambda Physik COMPex 205 excimer laser and a Coherent ScanMatePro dye laser. Frequency doubled radiation was focused on the molecular beam inside an ionization chamber between a repeller and extractor plates. Ions formed by multiphoton excitations were directed into a time-of-flight tube and detected by a micro-channel plates (MCPs) detector. Signals were fed into a LeCroy WaveSurfer 44MXs-A, 400 MHz storage oscilloscope and stored as a function of ion time-of-flights and laser radiation wavenumbers. Average signal levels were evaluated and recorded for a fixed number of laser pulses. The data were corrected for laser power and mass calibrated to obtain ion yields as a function of mass and excitation wavenumber (2D-REMPI data). REMPI spectra for certain ions as a function of excitation wavenumber (1D-REMPI) were obtained by integrating mass signal intensities for the particular ions. Care was taken to prevent saturation effects as well as power broadening by minimizing laser power. Laser calibration was based on observed (2 + 1) bromine atom REMPI peaks. The accuracy of the calibration was typically found to be about ±2.0 cm^{-1} on a two-photon wavenumber scale. Equipment condition parameters are listed in Table 1.

Table 1
Typical equipment/condition parameters for REMPI experiments.

HBr gas sample	Merck Schuchardt, Germany, Purity: 99.8%
Laser dyes	C480, C503, R540
Frequency doubling crystal	Sirah BBO-2
Laser repetition rate	10 Hz
Dye laser bandwidth	0.095 cm^{-1}
Laser intensity used	0.1–0.3 mJ/pulse
Nozzle size	500 μm
Sample backing pressure	2.0–2.5 bar
Pressure inside ionization chamber	10^{-6} mbar
Nozzle opening time	150–200 μs
Delay time for laser excitation	450–550 μs
Excitation wavenumber step sizes	0.05–0.1 cm^{-1}
Time of flight step sizes	10 ns

3. Results and analysis

Most HBr molecular spectra, previously detected in REMPI studies [21,26], in the two-photon resonance excitation region 74 000–86 000 cm^{-1} were identified and assigned. In addition, several "new spectra" were observed and assigned. These are grouped into three categories (see Table 2 and Fig. 1):

(i) Spectra due to two-photon resonance transitions to Rydberg states, not previously detected in REMPI but identified in single-photon absorption studies [9].
(ii) Spectra due to two-photon resonance transitions to Rydberg states, not previously detected.
(iii) Spectra due to two-photon resonance transitions to ion-pair states not previously detected or not analysed previously in terms of rotational energy structures.

Table 2 summarizes the above mentioned findings (i–iii). Fig. 1 shows some relevant 1D-REMPI spectra for parent and fragment ions. Spectra due to transitions to two Rydberg states ($k^3\Pi_1$ and $m^3\Pi_2$), not previously detected in REMPI, but identified in single-photon absorption studies [9], (i) are to be seen in Fig. 1a and b. Spectra due to transitions to two Rydberg states ($W^1\Sigma^+$ ($n = 6$, $v' = 0$) and $u^3\Delta_2$($n = 6$; $v' = 0$)) not previously detected, (ii) are to be seen in Fig. 1c and d and spectra due to transitions to the vibrational states of the $V^1\Sigma^+$ ion-pair state, $V(m + 18)$, $V(m + 19)$ and $V(m + 17)$, (iii) are to be seen in Fig. 1c–e respectively. The assignments and analysis of these spectra as well as two more vibrational bands, $V(m - 1)$ and $V(m + 12)$, (iii) will be dealt with in more detail below. In addition to the molecular REMPI spectra observed, several bromine atomic (2 + 1) REMPI resonances were identified. These are believed to be due to excitations of bromine atoms formed by predissociations of Rydberg states and/or following one-photon photodissociation via the repulsive state $A^1\Pi$ [39,47].

3.1. Spectra due to two-photon resonance transitions to Rydberg states, not previously detected in REMPI studies

By comparison with the analysis given by Ginter et al. [9] spectra centred at $v^0 = 80386.0$ cm^{-1} and 80644.0 cm^{-1} (Fig. 1a and b), which have not been seen in REMPI before, are assigned to two-photon resonance transitions to the $k^3\Pi_1$ ($v' = 0$) and $m^3\Pi_2$

Table 2
HBr: Band origin (v^0) and rotational parameters ($B'$and D') for the $k^3\Pi_1$ ($v' = 0$), $m^3\Pi_2$ ($v' = 0$), $W^1\Sigma^+$ ($n = 6$, $v' = 0$), $u^3\Delta_2$ ($v' = 0$), $V^1\Sigma^+$ ($m + 1$), $V^1\Sigma^+$ ($m + 12$), $V^1\Sigma^+$ ($m + 17$), $V^1\Sigma^+$ ($m + 18$) and $V^1\Sigma^+$ ($m + 19$) states.

State	n	v'	v^0		B'/cm^{-1}		$D' \times 10^3/cm^{-1}$		References for others' work
			Our work	Others' work	Our work	Others' work	Our work	Others' work	
$k^3\Pi_1$	5	0	80386.0	80386.0	8.150 ± 0.009	8.13	0.82	0.07	[9]
$m^3\Pi_2$	5	0	80644.0	80647.2	8.038 ± 0.017	8.05	−0.04	0.34	[9]
						8.04		0.23	
$W^1\Sigma^+$	6	0	85464.0	–	6.5 ± 0.1	–	4.4	–	–
$u^3\Delta_2$	6	0	85831.0	–	7.84 ± 0.05	–	0.3	–	–
$V^1\Sigma^+$	–	m − 1	75351.5	–	2.75 ± 0.16	–	−2.5	–	–
$V^1\Sigma^+$	–	m + 12	82416.7	82419.4[a]	4.12 ± 0.06	–	−32	–	[21]
				82417.9[b]			4.0		[21]
				82418					[9]
$V^1\Sigma^+$	–	m+17	85126.9	85027.1[a]	2.61 ± 0.11	–	9.3	–	[21]
				85027.3[b]					[21]
$V^1\Sigma^+$	–	m + 18	85598.4	–	4.02	–	34	–	–
$V^1\Sigma^+$	–	m+19	85918.6	–	3.23 ± 0.16	–	−1.8	–	–

[a] $H^{79}Br$.
[b] $H^{81}Br$.

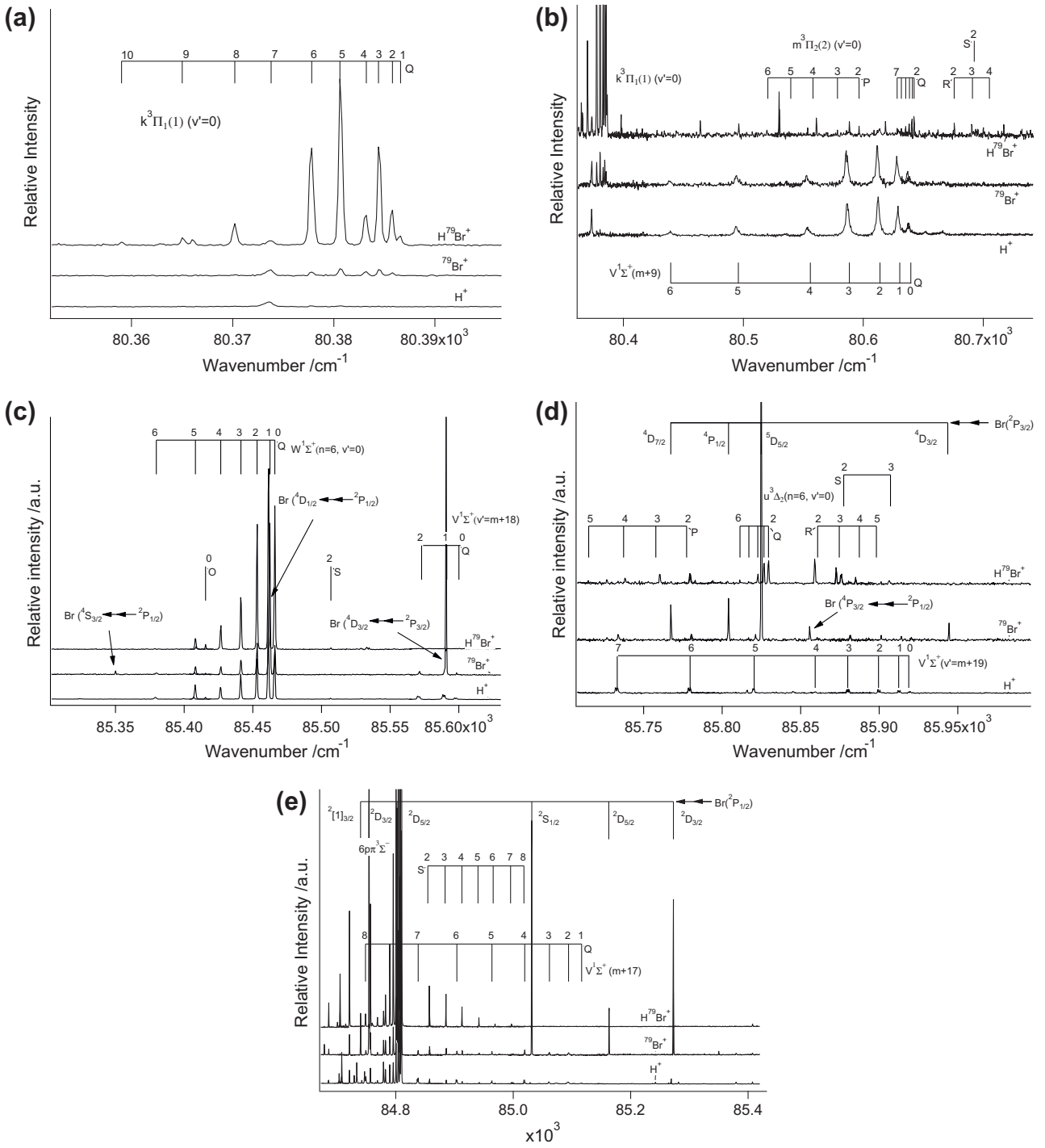

Fig. 1. 1D-REMPI spectra for H^+, $^{79}Br^+$ and $H^{79}Br^+$ and J' assignments of rotational peaks corresponding to two-photon resonance excitations to the $k^3\Pi_1$ ($v' = 0$) (a), $m^3\Pi_2$ ($v' = 0$) (b), $V^1\Sigma^+$ ($m + 9$) (b), $W^1\Sigma^+$ ($n = 6$, $v' = 0$) (c), $V^1\Sigma^+$ ($m + 18$) (c), $u^3\Delta_2$ ($n = 6$, $v' = 0$) (d), $V^1\Sigma^+$ ($m + 19$) (d) $6p\pi^3\Sigma^-$ ($v' = 0$) (e) and $V^1\Sigma^+$ ($m + 17$) (e) states. Bromine atomic (2 + 1) REMPI peaks are also marked.

($v' = 0$) Rydberg states respectively. Spectral analysis reveal rotational constants ($B'$and D') close to those given by Ginter et al. [9] (see Table 2).

Analogous to that observed by Ginter et al. perturbations are seen in the spectrum for $k^3\Pi_1$ ($v' = 0$) for $J' = 4$ and 7. This shows as line shifts, hence energy level shifts, as well as intensity alterations (see Fig. 1a). The intensity alterations show clearly as drops in the parent ion signals ($I(H^iBr^+)$) for $J' = 4$ and 7, but also as enhancements in the fragment ion signals ($I(^iBr^+)$ and I (H^+)), for $J' = 7$ in particular. Thus the intensity ratios $I(^iBr^+)/I(H^iBr^+)$ ($i = 79$, 81) as a function of J' show sharp peaks for $J' = 7$ and slight, but significant, increases for $J' = 4$ (see Fig. 2a). These observations are characteristic for near-resonance, level-to-level interactions between states with same J' values [43–47]. Large enhancement in the intensity ratio for $J' = 7$ is typical for a mixing of a Rydberg state with an ion-pair state, since ionization via an ion-pair state mainly results in fragment ions whereas ionization via pure, unmixed Rydberg states mainly results in parent ions. The Q line series for the ion-pair state $V(m + 9)$, seen in the fragment ion spectra only, shows broad peaks for $J' = 0$–6 on the long wavenumber side of the $k^3\Pi_1$

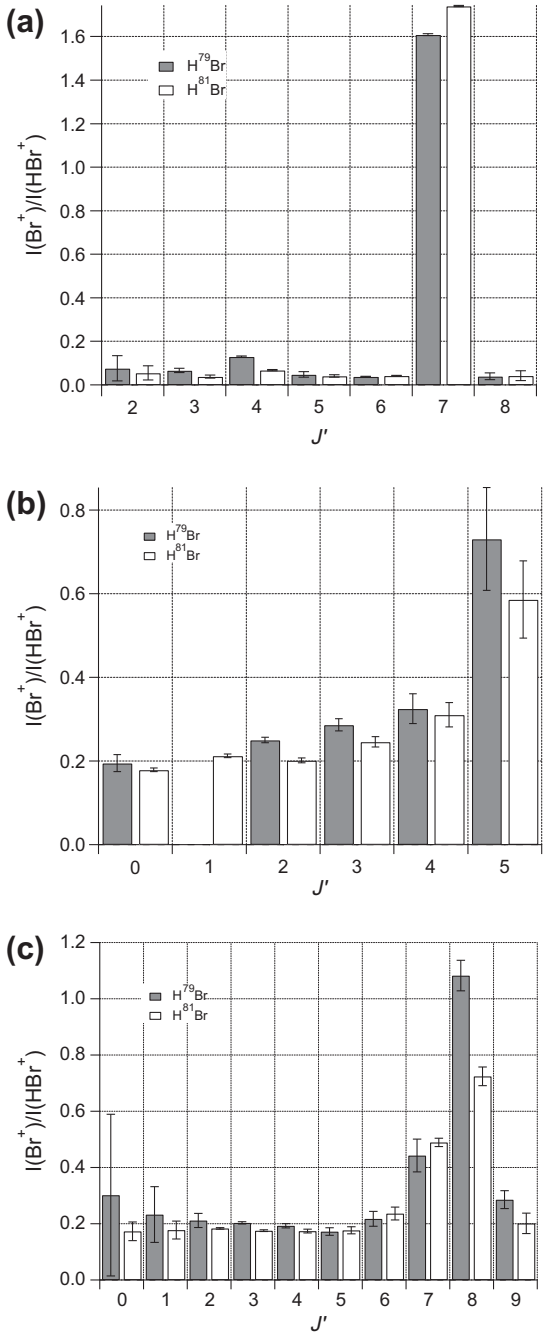

Fig. 2. Relative ion signal intensities, $I(^{i}Br^{+})/I(H^{i}Br^{+})$ (i = 79, 81) vs. J' derived from Q rotational lines of REMPI spectra due to two-photon resonance transitions to the Rydberg states $k^3\Pi_1$ (v' = 0) (a), $W^1\Sigma^+$ (n = 6, v' = 0) (b) and $6p\pi^3\Sigma^-$ (v' = 0) (c).

(v' = 0) spectrum (see Fig. 1b). Although the peak, for $V(m + 9)$, J' = 7 is too weak or too broad to be observed, an extrapolation of the Q line series suggests that it should be close to the Q lines for the $k^3\Pi_1$ (v' = 0) system, in which case the near-resonance interaction of concern must be between $k^3\Pi_1$ (v' = 0, J' = 7) and $V(m + 9; J' = 7)$. Thus an increased fragment ion signal and a decreased parent ion signal for the $k^3\Pi_1$ (v' = 0, J' = 7) resonance excitation is due to enhanced ion-pair state character in the mixed state. The state mixing, most probably is via $k^3\Pi_1$ and $k^3\Pi_0$ state interactions. The perturbation for J' = 4, on the other hand, mainly shows as a decrease in both signals (Fig. 1a) and small change in the intensity ratio, suggesting that it is not due to mixing with an ion-pair state. Most likely, therefore, it is due to mixing with another Rydberg state with lower ionization probability. There are no observed 1D-REMPI signals due to transitions to other Rydberg states, nearby, which could explain this, suggesting that it is a hidden state, i.e. a state not detectable in (2 + n) REMPI. This could be due to low transition probabilities or unfavorable selection rules. A possible candidate for a perturbing state is $i^3\Delta_3$ (v' = 1), which would be about 2100 cm^{-1} higher in energy than the v' = 0 vibrational component [21], as might be expected for an energy spacing between v' = 0 and v' = 1 for a Rydberg state. Coupling between the $i^3\Delta_3$ and the $k^3\Pi_1$ states could occur through the $i^3\Delta_2$ component, which can interact with $i^3\Delta_3$ by rotational coupling [27,43,47].

Table 3
Rotational lines for $H^{i}Br$ (i = 79, 81), due to two-photon resonance transitions to the $k^3\Pi_1$ (v' = 0), $m^3\Pi_2$ (v' = 0), $W^1\Sigma^+$ (n = 6, v' = 0), $u^3\Delta_2$ (n = 6, v' = 0), $V^1\Sigma^+$ (m + 1), $V^1\Sigma^+$ (m + 12), $V^1\Sigma^+$ (m + 17), $V^1\Sigma^+$ (m + 18) and $V^1\Sigma^+$ (m + 19) states.

J'	$k^3\Pi_1$	$m^3\Pi_2$			
	Q	P	Q	R	S
0					
1	80385.1				
2	80384.3	80596.5	80642.4	80676.0	80695.6
3	80383.1	80578.4	80640.8	80690.4	
4	80381.7	80558.0	80638.4	80704.8	
5	80379.3	80539.6	80635.4		
6	80376.4	80520.4	80631.7		
7	80372.3		80628.1		
8	80368.8				
9	80363.7				
10	80357.6				

	$W^1\Sigma^+$	$u^3\Delta_2$			
	Q	P	Q	R	S
0	85464.0				
1	85460.4				
2	85451.0	85777.2	85827.4	85856.9	85873.7
3	85439.3	85758.2	85824.5	85870.5	85903.5
4	85424.6	85736.1	85820.6	85882.8	
5	85406.1	85712.5	85814.9		
6	85377.7		85809.2		
7					
8					
9					
10					

	$V^1\Sigma^+$ (m − 1) Q	$V^1\Sigma^+$ (m + 12) Q	$V^1\Sigma^+$ (m + 17) Q	$V^1\Sigma^+$ (m + 18) Q ($H^{79}Br$)	$V^1\Sigma^+$ (m + 19) Q ($H^{79}Br$)
0	75351.5	82416.7		85598.4	85918.6
1	75342.2	82408.7	85114.5	85589.6	85912.1
2	75321.5	82393.1	85092.0	85571.2	85899.2
3	75287.9	82370.2	85059.5		85879.7
4	75241.8	82345.3	85017.5		85855.7
5	75186.3	82318.8	84961.7		85820.5
6	75124.0		84902.0		85779.4
7			84836.2		85732.6
8			84746.4		
9					
10					

The weak spectrum observed for $m^3\Pi_2$ (v' = 0) shows P, Q and R lines close to those observed by Ginter et al. [9] as well as the S line $J' = 2 \leftarrow\leftarrow J'' = 0$ (Table 3; Fig. 1b). In addition to $m^3\Pi_2$ (v' = 0) state peaks seen in that region some unidentified sharp peaks are also seen in the $H^{i}Br^{+}$ spectra in the region 80470–80620 cm^{-1} (Fig. 1b).

3.2. Spectra due to two-photon resonance transitions to Rydberg states, not previously detected

A spectrum, not previously observed, is seen in the two-photon excitation region 85370–85470 cm^{-1} (see Fig. 1c) with a

characteristic shape of a Q branch for a Rydberg state. It shows dominating HBr^+ signals but also significant fragment ion signals (Br^+ and H^+) with a varying intensity ratio $I(^iBr^+)/I(H^iBr^+)$ as a function of J' (see Fig. 2b). This is characteristic for an $\Omega = 0$ state showing strong homogeneous, off resonance, coupling with ion-pair vibrational states [45,47]. Spectral analysis, based on these assumptions, give rotational constant $B' = 6.50\ cm^{-1}$ and band origin $v^0 = 85463.0\ cm^{-1}$ (Table 2). This rotational constant is significantly lower than those for Rydberg states, which exhibit small or negligible couplings with ion-pair states, such as $\Omega > 0$ and triplet states and resembles values for the $E^1\Sigma^+$ state [21,26]. Extrapolation of known vibrational energies for the $E^1\Sigma^+$ ($n = 5$), $v' = 0$, 1, 2 and 3 states [21,26] reveals that this state cannot be a vibrationally excited E-state. Quantum defect analysis, on the other hand, gave similar quantum defect values, $\delta = 2.45$ and 2.40, for the $v^0 = 85463.0\ cm^{-1}$ and the $E^1\Sigma^+$ ($n = 5$, $v' = 0$) states, respectively in the expression,

$$v^0 = IE - R_H/(n-\delta)^2 \quad (1)$$

if $n = 6$ in the former case. IE is the ionization energy ($IE = 94205.52\ cm^{-1}$) and R_H is the Rydberg constant. We assign the $v^0 = 85463.0\ cm^{-1}$ state to $W^1\Sigma^+$ ($n = 6$, $v' = 0$). The intensity ratios, $I(^iBr^+)/I(H^iBr^+)$; $i = 79$, 81, gradually increase with J' for $J' = 0$–5 (Fig. 2b). This is typical for an increasing interaction as a function of J' with a higher lying $V(m + (i + 1))$ state and for a decreasing interaction as a function of J' with a lower lying $V(m + i)$ state, in a case where the interaction with the higher V state dominates [45]. That is the case when the higher energy V state ($V(m + (i + 1))$) is closer in energy to the Rydberg state (see Fig. 3). The V states of concern are $V(m + 17)$ and $V(m + 18)$ at $v^0 = 85102.0\ cm^{-1}$ and $85598.0\ cm^{-1}$, respectively, as discussed in more detail below. This interaction effect can also be seen from line-shifts, hence energy level shifts. The spacing between neighbor rotational levels ($\Delta E_{J'J'-1} = E(J') - E(J'-1)$) as a function of J', derived from the Q lines in the $W^1\Sigma^+$ ($n = 6$, $v' = 0$) spectrum (Fig. 1c) reveals negative deviation from linearity, which is typical for such off-resonance interactions [45,47].

The Rydberg spectrum shown in Fig. 1d shows only parent ion signals. Its rotational structure resembles number of hydrogen halide spectra for two-photon transitions to $\Omega = 2$ states [15–17,21,27]. Analysis based on that assumption gives $v^0 = 85831.0\ cm^{-1}$ and $B' = 7.84\ cm^{-1}$. This B' value is typical for a "pure", unperturbed Rydberg state. Furthermore, no significant perturbation effects are seen from line-shifts. Similar quantum defect parameters, $\delta = 2.35$ and $\delta = 2.38$, are obtained for the $i^3\Delta_2$ ($n = 5$, $v' = 0$) state at $v^0 = 78630.7\ cm^{-1}$ and this new state respectively, assuming the latter to be a $n = 6$ state. We assign this spectrum to transitions to the $u^3\Delta_2$ ($n = 6$, $v' = 0$) state.

3.3. Spectra due to two-photon resonance transitions to ion-pair states, not previously detected or analysed

Number of vibrational states of the $V^1\Sigma^+$ ion-pair state have been observed and identified [9,13,21,26]. Since the lowest energy vibrational states have not been observed the absolute vibrational quantum numbers, v', are uncertain. Therefore, it is customary to label the states as $V(v' = m + i)$ where i are positive integers ($i > 0$) and m is an unknown positive integer or zero. REMPI spectra have been observed and assigned to $V(m + i)$ states for $i = 1$–13, 15–17, 19, 22 [21,26]. The $V(m + i)$ ($i = 3$, 4, 6–11, 13, 15, 16, 19, 22) states have been analysed to determine rotational spectroscopic parameters [21,26]. $V(m + i)$ spectra are clearly distinguishable from Rydberg state spectra in (a) – showing larger red degradation of spectra bands to give lower rotational constants ($B' = 3.2$–$4.9\ cm^{-1}$) and in (b) – showing, typically, larger fragment ion signals than parent ion signals, hence intensity ratios $I(^iBr^+)/I(H^iBr^+) > 1$. Furthermore, (c) line-widths of ion-pair bands are often found to be larger than those for Rydberg spectra, close in energy [47]. This is clearly seen in Fig. 1b, which shows the spectrum for $V(m + 9)$ along with the spectra for the Rydberg states $k^3\Pi_1$ ($v' = 0$) and $m^3\Pi_2$ ($v' = 0$). (d) In contradiction with observations for Rydberg state spectra isotope splittings are sometimes seen in the $V(m + i)$ spectra. We now report detection of five $V(m + i)$ states ($i = -1$, 12, 17, 18 and 19), three of which, ($V(m - 1)$, $V(m + 18)$ and $V(m + 19)$), have not been detected before (see Table 2 and Fig. 1c and e). The REMPI spectra for $V(m + 12)$ and $V(m + 17)$ have not been analysed spectroscopically in detail, before. The spectrum for $V(m + 19)$ differs from the one assigned to $i = 19$, earlier [26], which has been reassigned accordingly.

A weak but clear ion-pair state spectrum is identified at $v^0 = 75353.0\ cm^{-1}$ (see Table 2). Spectra analysis reveal rotational constant $B' = 2.75\ cm^{-1}$, typical for an ion-pair state. Fragment ion signals ($^iBr^+$ and H^+) are found to be larger than parent ion signals. The wavenumber spacing (Δv^0) between this band origin and the next closest in energy, which has been observed ($V(m + 1)$; $v^0 = 76516.0\ cm^{-1}$ [21]) is $1163\ cm^{-1}$, which is about twice that to be expected between neighbor vibrational levels, v' and $v' - 1$. The vibrational energy spacing ($\Delta E_{v',v'-1} = E(v') - E(v'-1)$) in the $V^1\Sigma^+$ state is found to be irregular due to perturbations, ranging between about 400 and $600\ cm^{-1}$ for $i = 1$–8 [26]. This suggests that the new state is $V(m - 1)$. Calculations predict the band origin for $V(v' = 0)$ to be at $v^0 = 75548\ cm^{-1}$ [34] suggesting that this band could be due to transitions to $V(v' = 0)$ in which case $m = +1$. A search for a $V(m + 0)$ state spectrum in the excitation range between $75353\ cm^{-1}$ and $76516\ cm^{-1}$ was unsuccessful.

Few weak Q lines of an ion-pair state are seen for the fragment ion signals, slightly above the $W^1\Sigma^+$ ($n = 6$, $v' = 0$) spectrum (see Fig. 1c), as one would expect from the analysis of the W state, mentioned earlier. Small but clear isotope shift of about $1.4\ cm^{-1}$ is detected. Analysis reveal values of $v^0 = 85598.0\ cm^{-1}$ and $B' = 4.02\ cm^{-1}$ for this new state (Table 2). Judging from the observation of the $V(m + 17)$ state [21], which band origin is found, here, to be $v^0 = 85102.0\ cm^{-1}$ (see below) the energy spacing between this state and the $V(m + 17)$ state is $\Delta v^0 = 496\ cm^{-1}$, something to be expected for vibrational energy level spacing. This suggests that the new state is $V(m + 18)$.

Weak but clear ion-pair state spectra (Q lines) for $^iBr^+$ and H^+, with isotope splitting of about $1.1\ cm^{-1}$, are seen in the neighborhood of the $i^3\Delta_2$ ($n = 6$, $v' = 0$) state spectrum (Fig. 1d). Analysis reveal values of $v^0 = 85918.6\ cm^{-1}$ and $B' = 3.23\ cm^{-1}$ for this new state (Table 2). The energy spacing between this state and the $V(m + 18)$ state is about $\Delta v^0 = 320\ cm^{-1}$, suggesting that this spectrum is due to a transition to the $V(m + 19)$ state. The ion-pair state reported in Ref. [26] to be $V(m + 19)$ at $86314.7\ cm^{-1}$ therefore must be $V(m + 20)$. Furthermore, the state reported in the same reference as $V(m + 22)$ at $87607.5\ cm^{-1}$ therefore is more likely to be the $V(m + 23)$. The lower energy spacing between $V(m + 18)$ and $V(m + 19)$ of $320\ cm^{-1}$ compared to that between $V(m + 17)$ and $V(m + 18)$ ($496\ cm^{-1}$) is understandable because the strong state interactions between the $W(n = 6, v' = 0)$ state and the lower energy $V(m + 17)$ state and the higher energy $V(m + 18)$ state is repulsive in nature, resulting in an increased energy spacing between $V(m + 17)$ and $V(m + 18)$, hence decreasing spacing between $V(m + 18)$ and $V(m + 19)$.

Weak, broad, Q lines for the $V(m + 12)$ state are observed for the fragment ion signals, only. Analysis give $v^0 = 82417.0\ cm^{-1}$ and $B' = 4.12\ cm^{-1}$ (Table 2).

Relatively sharp Q lines, centred at $v^0 = 85102.0\ cm^{-1}$, are assigned to the $V(m + 17)$ state (Fig. 1e). Analysis give $B' = 1.31\ cm^{-1}$. This spectrum differs from that reported by Callaghan and Gordon ($v^0 \approx 85027\ cm^{-1}$ [21]). Further verification for our assignment is

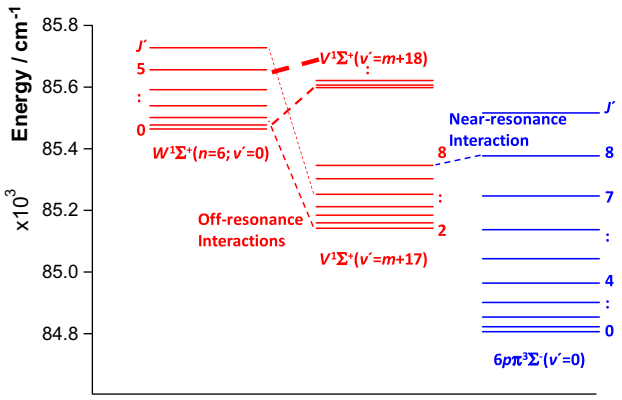

Fig. 3. Rotational energy levels, derived from observed REMPI rotational peaks for the $W^1\Sigma^+$ ($n = 6$, $v' = 0$), $V^1\Sigma^+$ ($m + 18$), $V^1\Sigma^+$ ($m + 17$) and $6p\pi^3\Sigma^-$ ($v' = 0$) states. Observed level-to-level near-resonance interaction between $6p\pi^3\Sigma^-$ ($v' = 0$) and $V^1\Sigma^+$ ($m + 17$) as well as off-resonance interactions between the ion-pair states ($V^1\Sigma^+$ ($m + 18$), $V^1\Sigma^+$ ($m + 17$)) and $W^1\Sigma^+$ ($n = 6$, $v' = 0$) are indicated by broken lines. Alterations in state mixings are indicated by varying thickness of broken lines.

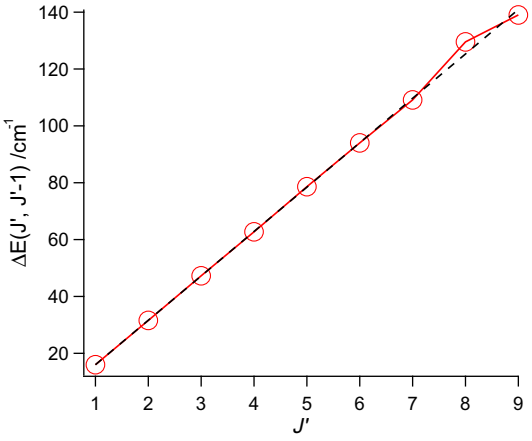

Fig. 4. Spacings between rotational levels ($\Delta E_{J'J'-1}$) as a function of J' for $6p\pi^3\Sigma^-$ ($v' = 0$). Dots connected by solid lines are derived from Q rotational lines. Broken line is linear fit for $J' = 1$–6.

evident from J'-dependent interaction found to occur between this state and the nearby $6p\pi^3\Sigma^-$ Rydberg state. Fig. 4 shows the spacing between neighbor rotational levels ($\Delta E_{J'J'-1} = E(J') - E(J' - 1)$) as a function of J' for the $6p\pi^3\Sigma^-$ state. The observed deviations in linearity of $\Delta E_{J'J'-1}$ for $J' = 7$, 8 and 9, with relatively large positive deviation for $J' = 8$ is typical for a near-resonance interaction [27,45,47] between $J' = 8$ levels, in which case the level for the $6p\pi^3\Sigma^-$ state is "pushed upward" due to an interaction from a lower lying $J' = 8$ state to make the energy spacing between levels $J' = 8$ and 7 ($\Delta E_{8,7}$) larger and $\Delta E_{7,6}$ and $\Delta E_{9,8}$ slightly smaller. The interaction of concern is a heterogeneous, $\Delta\Omega = 1$, interaction. This interaction is caused by the $J' = 8$ state of $V(m + 17)$, which Q line (84746.4 cm^{-1}) is found at slightly lower wavenumber than the Q ($J' = 8$) line for the $6p\pi^3\Sigma^-$ state (84777.2 cm^{-1}) (see Table 3 and Figs. 1e and 3). Furthermore, intensity ratios, $I(^iBr^+)/I(H^iBr^+)$, as a function of J' for the $6p\pi^3\Sigma^-$ state (see Fig. 2c), show clear evidence [43–47] for this near-resonance interaction, since the ratio reaches maximum for $J' = 8$.

4. Conclusions

Several new spectra features, observed in two-dimensional ($2 + n$) REMPI of H^iBr, were assigned and analysed. Rotational parameters and band origins were determined. Perturbation effects, seen as line-shifts and/or intensity anomalies, due to interactions between Rydberg states and ion-pair states and/or between two Rydberg states proved to be very helpful in assigning spectra. (i) Firstly, spectra due to resonance transitions to the Rydberg states $k^3\Pi_1$ ($v' = 0$) and $m^3\Pi_2$ ($v' = 0$), not previously observed in REMPI, were identified. Data revealed state interactions between the $k^3\Pi_1$ ($v' = 0$) state and the $V(m + 9)$ ion-pair state as well as between $k^3\Pi_1$ ($v' = 0$) and a hidden Rydberg state. (ii) Secondly, based on quantum defect analysis, two new spectra, not previously observed, were assigned to resonance transitions to the $W^1\Sigma^+$ ($n = 6$, $v' = 0$) and $u^3\Delta_2$ ($n = 6$, $v' = 0$) states. Effects of off-resonance interactions between the $W^1\Sigma^+$ ($n = 6$, $v' = 0$) state and the $V(m + 18)$ and $V(m + 17)$ states, further clarified the $W(n = 6, v' = 0)$ assignment. (iii) Thirdly, five vibrational bands of the ion-pair state $V^1\Sigma^+$, $V(m + i)$ ($i = -1$, 12, 17, 18 and 19), easily distinguishable from Rydberg state spectra, were identified and analysed. The spectra due to the transitions to $V(m - 1)$, $V(m + 18)$ and $V(m + 19)$ have not been detected before and those due to transitions to $V(m + 12)$ and $V(m + 17)$, have not been analysed spectroscopically before. The spectrum for $V(m + 17)$ was reassigned on the basis of observed near-resonance interaction with the $6p\pi^3\Sigma^-$ Rydberg state.

Acknowledgments

The financial support of the University Research Fund, University of Iceland, the Icelandic Science Foundation as well as the Norwegian Research Council is gratefully acknowledged.

References

[1] W.C. Price, Proc. Roy. Soc. Ser. A 167 (1938) 216.
[2] R.F. Barrow, J.G. Stamper, Proc. Roy. Soc. Ser. A. 263 (1961) 277–288.
[3] R.F. Barrow, J.G. Stamper, Proc. Roy. Soc. Ser. A. 263 (1961) 259–276.
[4] S.G. Tilford, M.L. Ginter, J.T. Vanderslice, J. Mol. Spectrosc. 33 (1970) 505–519.
[5] S.G. Tilford, M.L. Ginter, J. Molec, Spectroscopy 40 (1971) 568–579.
[6] D.S. Ginter, M.L. Ginter, J. Mol. Spectrosc. 90 (1981) 177–196.
[7] S.G. Tilford, M.L. Ginter, A.M. Bass, J. Mol. Spectrosc. 34 (1970) 327.
[8] M.L. Ginter, S.G. Tilford, A.M. Bass, J. Mol. Spectrosc. 57 (1975) 271.
[9] D.S. Ginter, M.L. Ginter, S.G. Tilford, J. Mol. Spectrosc. 90 (1981) 152.
[10] D.S. Ginter, M.L. Ginter, S.G. Tilford, A.M. Bass, J. Mol. Spectrosc. 92 (1982) 55.
[11] D.S. Ginter, M.L. Ginter, S.G. Tilford, J. Mol. Spectrosc. 92 (1982) 40.
[12] J.B. Nee, M. Suto, L.C. Lee, J. Chem. Phys. 85 (1986) 719–724.
[13] J.B. Nee, M. Suto, L.C. Lee, J. Chem. Phys. 85 (1986) 4919.
[14] T.A. Spiglanin, D.W. Chandler, D.H. Parker, Chem. Phys. Lett. 137 (5) (1987) 414–420.
[15] D.S. Green, G.A. Bickel, S.C. Wallace, J. Mol. Spectrosc. 150 (2) (1991) 303–353.
[16] D.S. Green, G.A. Bickel, S.C. Wallace, J. Mol. Spectrosc. 150 (2) (1991) 354–387.
[17] D.S. Green, G.A. Bickel, S.C. Wallace, J. Mol. Spectrosc. 150 (2) (1991) 388–469.
[18] D.S. Green, S.C. Wallace, J. Chem. Phys. 96 (8) (1992) 5857–5877.
[19] E.d. Beer, B.G. Koenders, M.P. Koopmans, C.A.d. Lange, J. Chem. Soc. Faraday Trans. 86 (11) (1990) 2035–2041.
[20] Y. Xie, P.T.A. Reilly, S. Chilukuri, R.J. Gordon, J. Chem. Phys. 95 (2) (1991) 854–864.
[21] R. Callaghan, R.J. Gordon, J. Chem. Phys. 93 (1990) 4624–4636.
[22] Á. Kvaran, H. Wang, Á. Logadóttir, Rotational REMPI Spectroscopy; Halogen containing Compounds, in: Recent Res. Devel. in Physical Chem. 1998, Transworld Research, Network, pp. 233–244.
[23] S.A. Wright, J.D. McDonald, J. Chem. Phys. 101 (1) (1994) 238–245.
[24] S.T. Pratt, M.L. Ginter, J. Chem. Phys. 102 (1995) 1882–1888.
[25] E.d. Beer, W.J. Buma, C.A. deLange, J. Chem. Phys. 99 (5) (1993) 3252–3261.
[26] Á. Kvaran, Á. Logadóttir, H. Wang, J. Chem. Phys. 109 (14) (1998) 5856–5867.
[27] Á. Kvaran, H. Wang, Á. Logadóttir, J. Chem. Phys. 112 (24) (2000) 10811–10820.
[28] Á. Kvaran, B.G. Waage, H. Wang, J. Chem. Phys. 113 (5) (2000) 1755–1761.
[29] D. Ascenzi, S. Langford, M. Ashfold, A. Orr-Ewing, Phys. Chem. Chem. Phys. 3 (1) (2001) 29–43.
[30] R. Liyanage, R.J. Gordon, R.W. Field, J. Chem. Phys. 109 (19) (1998) 8374–8387.
[31] M. Bettendorff, S.D. Peyerimhoff, R.J. Buenker, Chem. Phys. 66 (1982) 261–279.
[32] D.M. Hirst, M.F. Guest, Mol. Phys. 41 (6) (1980) 1483–1491.
[33] H. Lefebvre-Brion, H.P. Liebermann, G.J. Vazquez, J. Chem. Phys. 134 (20) (2011) 204104.
[34] S.Z. Zlatkova, Computational investigation of the ionization and photo-ionizationof hydrogen halide acids in water clusters, in: The Department of

Chemistry and Biochemistry, Concordia University Montreal, Quebec, 2006, p. 100.
[35] A.I. Chichinin, C. Maul, K.H. Gericke, J. Chem. Phys. 124 (22) (2006) 224324.
[36] A.I. Chichinin, P.S. Shternin, N. Godecke, S. Kauczok, C. Maul, O.S. Vasyutinskii, K.H. Gericke, J. Chem. Phys. 125 (3) (2006) 034310.
[37] S. Kauczok, C. Maul, A.I. Chichinin, K.H. Gericke, J. Chem. Phys. 133 (2) (2010) 24301.
[38] C. Maul, S. Kauczok, V. Werwein, K.-H. Gericke, The unusual behaviour of the F(1D2) state of HCl: A 3 D Velocity Map Imaging Study, in: The 21st Colloquium on High Resolution Molecular Spectroscopy International Conference, Castellammare di Stabia (Italy), 2009.
[39] C. Romanescu, H.P. Loock, Phys. Chem. Chem. Phys. 8 (25) (2006) 2940–2949.
[40] C. Romanescu, H.P. Loock, J. Chem. Phys. 127 (12) (2007) 124304.
[41] C. Romanescu, S. Manzhos, D. Boldovsky, J. Clarke, H. Loock, J. Chem. Phys. 120 (2) (2004) 767–777.
[42] Kristján Matthíasson, J. Long, Huasheng Wang, A. Kvaran, J. Chem. Phys. 134 (2011) 164302.
[43] A. Kvaran, H.S. Wang, K. Matthiasson, A. Bodi, E. Jonsson, J. Chem. Phys. 129 (16) (2008) 164313.
[44] A. Kvaran, K. Matthiasson, H.S. Wang, J. Chem. Phys. 131 (4) (2009) 044324.
[45] K. Matthiasson, J.M. Long, H.S. Wang, A. Kvaran, J. Chem. Phys. 134 (16) (2011) 164302.
[46] K. Matthiasson, H.S. Wang, A. Kvaran, J. Mol. Spectrosc. 255 (1) (2009) 1–5.
[47] J.M. Long, H.R. Hrodmarsson, W.H. Wang, A. Kvaran, J. Chem. Phys. 136 (2012) 214315.
[48] Á. Kvaran, H. Wang, Mol. Phys. 100 (22) (2002) 3513–3519.
[49] Á. Kvaran, K. Matthíasson, H. Wang, Phys. Chem.: Indian J. 1 (1) (2006) 11–25.
[50] Á. Kvaran, Ó.F. Sigurbjörnsson, H. Wang, J. Mol. Struct. 790 (2006) 27–30.